Upconversion emission in a carbon-implanted Yb:YAG planar waveguide

G.V. Vázquez [a,*], H. Desirena [a], E. De la Rosa [a], E. Flores-Romero [b], H. Márquez [c], J. Rickards [b], R. Trejo-Luna [b]

[a] Centro de Investigaciones en Óptica, A.P. 1-948, León, Gto. 37150, Mexico
[b] Instituto de Física, UNAM, Apartado Postal 20364, México, D.F. 01000, Mexico
[c] Departamento de Óptica, CICESE, km 107 Carr. Tijuana-Ensenada, 22860 Ensenada, B.C., Mexico

ABSTRACT

Light confinement and spectroscopic properties of a Yb:YAG planar waveguide fabricated by ion implantation were investigated. Under 970 nm excitation, cooperative upconversion and near infrared luminescence were observed. The interaction between Yb^{3+} ion pairs was responsible for the appearance of a blue–green band centered at 514 nm. However, several more bands in the blue, green and red regions were detected and are related to Er^{3+} and Tm^{3+} ion impurities. The upconversion emission of such ion impurities is explained in terms of an efficient energy transfer from Yb^{3+} to Er^{3+} and Tm^{3+} due to high Yb^{3+} concentration. The stimulated emission cross section for the $^2F_{5/2} \rightarrow {}^2F_{7/2}$ transition of Yb^{3+} was 1.9×10^{-20} cm^2. The fluorescence lifetime of the $^2F_{5/2}$ level and that of the blue–green band were 1.28 ms and 593 μs respectively. The self-convolution of IR emission was calculated and the result shows that the main peak is centered at 514 nm. Such self-convolution and the fact that the blue–green band lifetime is half the IR lifetime are good evidences for cooperative emission of Yb^{3+} ion pairs.

1. Introduction

The Yb:YAG crystal is important in near infrared (NIR) lasers; it has a broad absorption band, from about 900 to 1050 nm, which is well suited for diode pumping; it also has a fluorescence lifetime of about 1 ms without a significant reduction even for high doping levels (> 20 at% [1]), can be achieved because of the excellent coupling between the ytterbium radius and that of the yttrium. It exhibits a very simple electronic level structure, with the ground state ($^2F_{7/2}$) and one excited state manifold ($^2F_{5/2}$). All these properties offer advantages over the widely used Nd:YAG crystal. Combining these characteristics with a waveguide configuration provides low pump power thresholds and high optical efficiencies, which is of great importance in laser applications [2–5].

In order to have high laser performance, special care must be taken in the Yb^{3+} doped crystal processing, since non-radiative energy losses due to impurities that enter during crystal growth can reduce the stored energy and thereby affect the laser gain. The electronic configuration of Yb^{3+} ions makes the 4f electrons less shielded than in other ions of the lanthanide series, showing a higher tendency to interact with the lattice and neighbor ions. These characteristics make Yb^{3+} an excellent sensitizer for most

of the rare earths (RE). Specifically, a luminescence process takes place when the $^2F_{5/2} \rightarrow {}^2F_{7/2}$ transition of Yb^{3+} and ground to excited level transitions of other RE are resonant. This process is the well known energy transfer (ET). Lanthanides such as Er^{3+}, Pr^{3+}, Ho^{3+}, Dy^{3+}, Tm^{3+} and Sm^{3+} have a similar energy gap to Yb^{3+} and the combination of such ions will generate energy transfer [6–12]. On the other hand, when the Yb^{3+} concentration is high, a new phenomenon appears and is called cooperative upconversion. Such phenomenon has been explained in terms of the relaxation of a virtual state created by the simultaneous excitation of two Yb^{3+} ions forming an ionic pair (Yb–Yb interaction), which subsequently emits a photon with the sum of energies, leading to blue–green emission. Cooperative emission has been observed previously in Yb^{3+} doped materials [6–9], particularly in the YAG host in waveguide configuration [10] and nanocrystals [11]. In addition, this process was observed in bulk YAG where impurities of other RE ions were found, leading to the appearance of several upconversion luminescence bands [12]. Both ET and cooperative upconversion are drawbacks that reduce the laser performance at 1.03 μm, and hence, these processes should be minimized. In this sense, knowing the energy loss channels is an important issue that should be considered in the design of a NIR laser. However, from another point of view, the presence of visible emission as a result of the upconversion process can be used in the design of lasers with visible emission and displays.

* Corresponding author. Tel.: +52 477 4 41 42 00x273; fax: +52 477 4 41 42 09.
E-mail address: gvvazquez@cio.mx (G.V. Vázquez).

In this work, we report results on cooperative emission of Yb^{3+} ions in a YAG host where a waveguide was fabricated by ion implantation. Blue, green and red emissions were observed and are associated with the traces of Er^{3+} and Tm^{3+} ions. Fluorescence lifetime of both the $^2F_{5/2} \rightarrow ^2F_{7/2}$ transition and blue–green band of Yb^{3+} was measured. The self-convolution of the infrared emission spectrum was calculated and the results show that it matches very well with the cooperative upconversion emission. Results include distribution of propagating modes, absorption and luminescence curves, as well as fluorescence lifetimes and emission cross section.

2. Experimental methods

By ion implantation a planar waveguide was fabricated on a commercial 5 at% Yb:YAG crystal (Foctek Photonics) with dimensions of $15 \times 10 \times 1$ mm^3 using carbon ions at an energy of 7 MeV and a dose of 7×10^{14} ions/cm^2. Optical microscopy measurements of the implanted region were done to estimate the waveguide thickness. The intensity distribution of the propagating modes was obtained using a pigtailed fiber laser operating at 635 nm as the source and a CCD camera was located at the output of the waveguide.

For the spectroscopic study, a diode laser operating at 970 nm was used to excite the Yb^{3+} ions in both the NIR and the visible (VIS) region. A $10 \times$ objective lens was used to couple the pump light into the waveguide. The luminescence from the waveguide was collected using an optical fiber and directed onto a monochromator (Acton Research SP-2357); the NIR emission was detected by an InGaAs detector (Thorlabs DET10C) and the VIS emission by a photomultiplier tube (Acton Research PD471). The temporal evolution was recorded at 514 and 1030 nm using an SR540 chopper (Stanford Research System); the signal was synchronously detected and averaged by a digital oscilloscope (Tektronix TDS3052B). Measurements were also taken in the bulk crystal in order to see any effect of the implantation process on the spectroscopic properties of the waveguide region. The absorption spectrum was recorded by a Perkin–Elmer spectrophotometer in the perpendicular direction of the waveguide, hence, the absorption corresponds to both waveguide and bulk crystal.

3. Results and discussion

According to the simulated ion range using the Stopping and Range of Ions in Matter (SRIM) program [13], the waveguide thickness was calculated to be ~ 4.5 μm and is located in a 15×10 mm^2 surface area; this was confirmed by optical microscopy measurements. Fig. 1a shows an image of the crystal where the planar waveguide can be observed with different color in the crystal–air interface. Fig. 1b shows the intensity distribution of
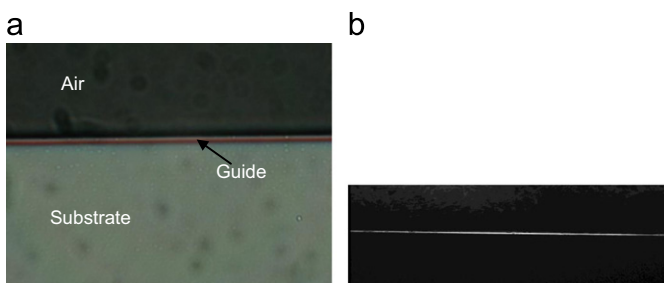
the propagating modes at the waveguide output, confirming light confinement in the vertical direction (i.e., a planar waveguide). It is worth to mention that the propagation loss in the waveguide is ~ 10 dB/cm [2] which can be reduced by an annealing treatment; previous results of Nd:YAG waveguides have shown similar or lower losses and laser oscillation was achieved on these structures [14,15].

The NIR absorption spectrum of 5 at% Yb^{3+} in YAG is shown in Fig. 2. It exhibits the characteristic broad band of ytterbium ions and corresponds to the $^2F_{7/2} \rightarrow ^2F_{5/2}$ transition with a wavelength range from 860 to 1060 nm. The spectrum shows a shoulder around 912 nm and three clear peaks can be identified; the main one is located at around 935 nm, followed by the second peak centered at 965 nm. The shortest peak at 1026 nm corresponds to the transition related to the typical emission of Yb^{3+} (~ 1.03 μm). The inset of Fig. 2 shows the absorption curve in the visible region recorded from 450 to 750 nm. No absorption bands can be seen, contrary to several reports where cooperative emission was accompanied by cooperative absorption [9,11].

Fig. 3 shows the emission spectrum obtained from the waveguide in the NIR region at room temperature. The NIR emission corresponds to the typical broad-band spectrum of Yb^{3+} ions in YAG centered at 1028 nm with a band ranging from 900 to 1100 nm (black short-dotted line). Such broad band (~ 200 nm) is very useful for tunable laser applications. In fact, several works on Yb^{3+} doped materials have reported tunable laser emission. Petit et al. have obtained a 60 nm tunable laser in a Yb^{3+} doped CaF_2 crystal [16], and recently, Hao et al. have reported generation of 68 nm tunability in an Yb^{3+} doped yttrium lanthanum oxide ceramic [17]. It should be noted that the sample reported in the present work was consciously doped with Yb^{3+} and not with other rare earths; however several bands in the blue, green and red region (blue solid line) were observed. These bands are related to the presence of other rare earth ions such as Er^{3+} and Tm^{3+}. According to the Dieke diagram [18] and reported data on the position of the stark energy levels [19], the blue emission bands centered at 460, 472, 477, 486 and a shoulder at 493 nm are associated with the transition $^1G_4 \rightarrow ^3H_6$ of Tm^{3+} ions. From Fig. 3, it can be seen that the peak centered at 486 nm is the strongest emission among the aforementioned bands. Such peak coincides with the main emission reported previously in YAG bulk crystals that were consciously doped with Tm^{3+} ions [20,21]. The blue bands peaked at 499 and 502 nm correspond to the $^4F_{7/2} \rightarrow ^4I_{15/2}$ transition of Er^{3+}; the $^2H_{11/2} \rightarrow ^4I_{15/2}$ Er^{3+} transition is assigned to the bands centered at 519 and 524 nm; and the

Fig. 1. (a) Image by optical microscopy of the implanted crystal showing a section of the planar waveguide; (b) field pattern of the propagating modes in the waveguide.
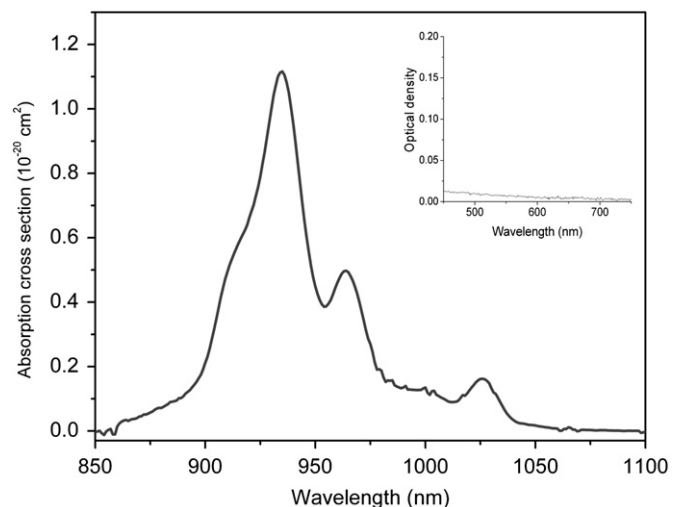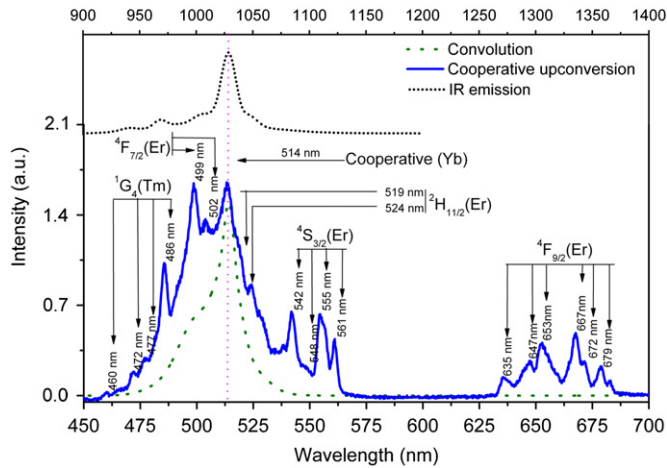

Fig. 2. Absorption spectrum of the 5 at% Yb^{3+} in YAG.

Fig. 3. NIR emission spectrum of the Yb:YAG waveguide (black short-dotted line), cooperative luminescence spectrum of Yb^{3+} ions (blue continuous line), and self-convolution of the infrared emission spectrum (green dotted line). (For interpretation of the references to color in this figure legend, the reader is referred to the web version of this article.)

Fig. 4. Fluorescence decay of the NIR emission (red circles) and cooperative luminescence (blue squares) for Yb^{3+} ions in YAG. (For interpretation of the references to color in this figure legend, the reader is referred to the web version of this article.)

$^4S_{3/2} \rightarrow {}^4I_{15/2}$ transition caused the green luminescence between 538 and 561 nm. The red bands centered at around 667 nm are the contributions of the transition $^4F_{9/2} \rightarrow {}^4I_{15/2}$ of Er^{3+} ions and $^1G_4 \rightarrow {}^3H_4$ of Tm^{3+} ions. Indeed, rare earth elements are closely related chemically, and thus, they are very difficult to separate from each other. This is the reason that some traces of Er^{3+}, Tm^{3+} or other rare earths are generally found in Yb^{3+} doped solids. Let us remind that such traces are unquantifiable under absorption spectroscopy as can be observed in the inset of Fig. 2. The energy transfer from Yb^{3+} to these traces is very efficient at these concentrations and the reason is as follows: the Yb^{3+} concentration is around 7×10^{20} cm^{-3} (the Yb_2O_3 purity is $\sim$99.9995%), while Er^{3+} and Tm^{3+} concentrations are about 10^{17} cm^{-3}, which means three orders of magnitude lower than Yb^{3+}. Therefore, the probability of several Yb^{3+} ions surrounding an impurity ion (Er^{3+} and Tm^{3+}) is very large. Direct excitation to Er^{3+} is also possible; however, energy transfer is most probably due to the larger absorption cross section of Yb^{3+} and is quasi-resonant between the $^2F_{5/2} \rightarrow {}^2F_{7/2}$ and $^4I_{15/2} \rightarrow {}^4I_{11/2}$ transition of Yb^{3+} and Er^{3+}, respectively. In the case of Tm^{3+}, the $^3H_6 \rightarrow {}^3H_4$ transition is not resonant; however this occurs under Stokes excitations, as has been reported in Refs. [22–24]. The overall results lead to very efficient energy transfer from the Yb^{3+} ions to Er^{3+} and Tm^{3+} and the consequent upconversion luminescence of the impurity ions. Finally, an intense peak at 514 nm was also recorded and is attributed to a cooperative process between Yb^{3+} ion pairs. There are some evidences confirming that this peak corresponds to cooperative upconversion. The first one is that the energy of this peak is 19,455 cm^{-1} and does not match with any energy level of Er^{3+} or Tm^{3+}. The second one is the self-convolution of the NIR emission, which is shown in Fig. 3 (green dotted line). The peak corresponds to twice the energy of the infrared emission and it matches well with the peak position of the cooperative emission at 514 nm. This correspondence is one of the best evidence showing that this energy band is attributed to cooperative upconversion of Yb^{3+} pairs.

Additional evidence that supports our assumption about cooperative upconversion emission is the measured fluorescence lifetime. According to previous results, the cooperative luminescence lifetime of Yb^{3+} ions should be half the lifetime of the infrared transition. This is because the population is reduced to a half since the cooperative phenomenon is the result of the formation of Yb^{3+} ion pairs [7,10]. Fig. 4 shows the NIR and VIS
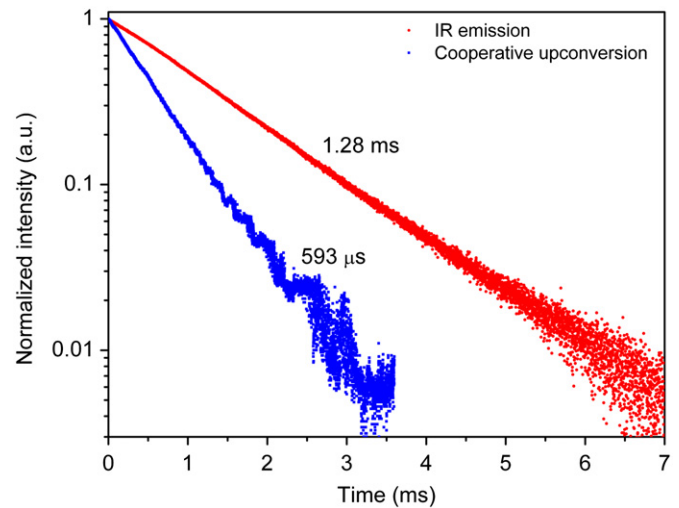
temporal evolution of the Yb^{3+} ions. For the infrared transition (red circles), the luminescence decay time was calculated to be $\sim$1.28 ms, in accordance with previous reports of bulk 5 at% Yb:YAG [1,12]. For the cooperative fluorescence decay (blue squares), a lifetime value of $\sim$593 μs was obtained, which is approximately half of the lifetime in the NIR region.

It is important to note that the emission spectra and temporal evolution were similar in the bulk and waveguide area, which means that the carbon implantation used to form the planar waveguide did not affect the spectroscopic properties of the material in the guiding region, including the effects of cooperative emission and energy transfer. According to experimental results reported here, upconversion emission of Er^{3+} and Tm^{3+} ions and the cooperative emission of Yb^{3+} pairs are the result of ion interaction and are not dependent on the presence of implanted carbon or the confinement effect related to the guiding process. Previous works have shown that heavy ion (e.g., carbon) implanted waveguides maintain the spectroscopic properties of the original material [25,26].

Using the fluorescence spectrum and radiative lifetime, we also obtained the stimulated emission cross section as this is an important parameter when assessing the properties of a laser crystal, particularly in a waveguide configuration. Laser performance parameters such as the threshold pump power depend on this value; any reduction on the emission cross section will produce a higher laser threshold. We calculated the stimulated emission cross section of the Yb:YAG crystal from the measured emission line shape using the Fuchtbauer–Ladenburg formula [27]:

$$\sigma_{emi}(\lambda_p) = \frac{\lambda_p^4 A}{8\pi c\, n^2\, \Delta\lambda_{eff}} \qquad (1)$$

where λ_p is the peak fluorescence wavelength, c the speed of light, n the refractive index and A is the radiative transition probability of the $^2F_{5/2} \rightarrow {}^2F_{7/2}$ transition of Yb^{3+}, which is inversely proportional to the radiative lifetime, $A = 1/\tau_{rad}$. According to several reports, the radiative lifetime τ_{rad} is lower than the measured lifetime value because of the effect of radiation trapping [1,28]. This effect is stronger as the sample thickness increases. The value of radiative lifetime used for the calculation was 0.95 ms [28]. $\Delta\lambda_{eff}$ is an effective linewidth which results from a slight asymmetry in the emission band and is

determined using the following expression:

$$\Delta\lambda_{eff} = \int \frac{I(\lambda)}{I_p} d\lambda \qquad (2)$$

where I_p is the peak fluorescence intensity corresponding to λ_p. The maximum value calculated for the emission cross section was $1.93 \times 10^{-20}\,cm^2$, which is in good agreement with the results reported previously [28,29].

In our case, the cooperative luminescence between Yb^{3+} ions and the energy transfer caused by the presence of RE traces in the YAG crystal are mechanisms which lead to fluorescence quenching of the Yb^{3+} $^2F_{5/2} \rightarrow {}^2F_{7/2}$ transition. A reduction in the decay time of this Yb^{3+} NIR transition is expected, which in turn is related to a decrease in the quantum efficiency of the system. Therefore, the final outcome of the upconversion emission in the Yb:YAG waveguide impacts the NIR laser performance; a solution will be taking special care during the crystal growth in order to obtain highly pure substrate materials for waveguide fabrication. On the other hand, it is important to point out that RE ion co-doping in the YAG host together with a waveguide configuration could mean an important step in designing a compact upconversion laser.

4. Conclusions

Upconversion luminescence was measured in a carbon implanted Yb:YAG planar waveguide. The phenomenon corresponds to a cooperative interaction between ytterbium ion pairs as well as energy transfer from Yb^{3+} ions to erbium and thulium impurities present in the crystal lattice. The results are important to quantify the energy deviated from the main NIR transition of Yb^{3+} ions, which represents a negative effect in the efficiency of laser devices.

Acknowledgments

References

[1] J. Dong, M. Bass, Y. Mao, P. Deng, F. Gan, Journal of Optical Society of America B 20 (2003) 1975.

[2] G.V. Vázquez, D. Ramírez, H. Márquez, E. Flores-Romero, J. Rickards, R. Trejo-Luna, Applied Optics 51 (2012) 5573.

[3] A. Benayas, W. Da Silva, A. Ródenas, C. Jacinto, J.R. Vázquez de Aldana, F. Chen, Y. Tan, R. Thomson, A. Kar, N. Psila, D. Reid, D. Jaque, Applied Physics A 104 (2011) 301.

[4] I.J. Thomson, F.J.F. Monjardin, H.J. Baker, D.R. Hall, IEEE Journal of Quantum Electronics 47 (2011) 1336.

[5] E. Cantelar, D. Jaque, G. Lifante, Optical Materials 34 (2012) 555.

[6] E. Nakazawa, S. Shionoya, Physical Review Letters 25 (1970) 1710.

[7] F. Auzel, D. Meichenin, F. Pelle, P. Goldner, Optical Materials 4 (1994) 35.

[8] E. Montoya, O. Espeso, L.E. Bausá, Journal of Luminescence 87–89 (2000) 1036.

[9] A.V. Kir'yanov, Y.O. Barmenkov, I. Lucio-Martínez, A.S. Kurkov, E.M. Dianov, Optics Express 14 (2006) 3981.

[10] M. Malinowski, M. Kaczkan, R. Piramidowicz, Z. Frukacz, J. Sarnecki, Journal of Luminescence 94–95 (2001) 29.

[11] L.A. Diaz-Torres, E. De la Rosa, P. Salas, H. Desirena, Optical Materials 27 (2005) 1305.

[12] X. Xu, Z. Zhao, P. Song, B. Jiang, et al., Physica B 357 (2005) 365.

[13] ⟨http://www.srim.org⟩, last accessed November 2011.

[14] M. Domenech, G.V. Vázquez, E. Cantelar, G. Lifante, Applied Physics Letters 83 (2003) 4110.

[15] G.V. Vázquez, H. Márquez, E. Flores-Romero, M.E. Sánchez-Morales, in: R. Espinosa-Luna, E. Bernabeu (Eds.), Recent Research in Photonics, Research Signpost, India, 2009, pp. 153–181.

[16] V. Petit, J.L. Doualan, P. Camy, V. Menard, R. Moncorge, Applied Physics B 78 (2004) 681.

[17] Q. Hao, W. Li, H. Zeng, Q. Yang, C. Dou, H. Zhou, W. Lu, Applied Physics Letters 92 (2008) 211106.

[18] G.H. Dieke, Spectra and Energy Levels of Rare Earth Ions in Crystals, Wiley Interscience, New York, 1968.

[19] A.A. Kaminskii, Laser Crystals: Their Physics and Properties, Springer Verlag, New York, 1990.

[20] W. Xu, X. Xu, F. Wu, G. Zhao, Z. Zhao, G. Zhou, J. Xu, Optics Communications 272 (2007) 182.

[21] M. Szachowicz, P. Moretti, M.F. Joubert, M. Couchaud, B. Ferrand, Applied Physics Letters 90 (2007) 031113.

[22] W.F. Silva, G.S.N. Eliel, P.V. dos Santos, M.T. de Araujo, M.V.D. Vermelho, P.T. Udo, N.G.C. Astrath, M.L. Baesso, C. Jacinto, Journal of Chemical Physics 133 (2010) 034507.

[23] C.J. da Silva, M.T. de Araujo, E.A. Gouveia, A.S. Gouveia-Neto, Applied Physics B 70 (2000) 185.

[24] C.J. da Silva, M.T. de Araujo, E.A. Gouveia, A.S. Gouveia-Neto, Optics Letters 24 (1999) 1287.

[25] M.E. Sánchez Morales, G.V. Vázquez, H. Márquez, J. Rickards, R. Trejo-Luna, Journal of Modern Optics 53 (2006) 539.

[26] E. Flores-Romero, G.V. Vázquez, H. Márquez, R. Rangel-Rojo, J. Rickards, R. Trejo-Luna, Optics Express 15 (2007) 8513.

[27] J.F. Philipps, T. Topfer, H. Ebendorff-Heidepriem, D. Ehrt, R. Sauerbrey, Applied Physics B 72 (2001) 399.

[28] D.S. Sumida, T.Y. Fan, OSA Proceedings on Advanced Solid State Lasers 20 (1994) 100.

[29] B.-X. Jiang, T.-D. Huang, Y.-S. Wu, W.- Liu, Y.-B. Pan, T. Feng, Q.-H. Yang, Chinese Physics B 17 (2008) 3407.